euronoise

Numerical computation of reflected and transmitted waves at a fluid/solid interface

Laure Bossy[a,b], Marie-Françoise Cugnet[a], Emmanuel Bossy[c] and Didier Cassereau[b]

[a]AREVA - CEZUS Research Center, Avenue Paul Girod, 73403 Ugine Cedex, France
[b]Laboratoire Ondes et Acoustique, 10, rue Vauquelin, 75231 Paris, France
[c]Laboratoire Photons et Matière, ESPCI/CNRS, 10 rue Vauquelin, 75231 Paris Cedex 05, France
laure.bossy@espci.fr

In this paper, we propose a numerical computation of the different waves generated when a spherical incident pulse is reflected and transmitted by a fluid/solid interface. In addition to the standard reflected and transmitted waves that propagate inside the volume, various surface waves can also be found in both propagation media. In the fluid, we can observe the longitudinal and transverse head waves, and the so-called leaky Rayleigh wave that generalizes the Rayleigh wave in a semi-infinite free solid medium to the case of an immersed interface. Similar effects can also be observed on the transmitted displacement field inside the solid material. We compare different numerical approaches, including semi-analytic methods (high-frequency approximation coupled to ray modeling approach) and implicit methods (finite elements and/or finite differences scheme), each method having its own advantages and inconvenients, and domains of validity. These different methods are used to evaluate the field reflected by the interface ; the transmitted displacement field is also analyzed from the same point of view.

1 Introduction

In this paper, we are interested in the different contributions that appear when a spherical wave is reflected by an immersed solid material. In addition to the well known specular reflection, we can also observe head waves corresponding to the longitudinal and transverse waves generated in the solid, and also the so-called leaky Rayleigh wave that generalizes the Rayleigh wave in a semi-infinite free solid medium to the case of an immersed interface. These different contributions correspond to surface waves that propagate along the fluid/solid interface and permanently radiate some energy back in the fluid. At the Rayleigh angle, a distortion of the reflected wavefront appears, that corresponds to a fast variation of the reflection coefficient with respect to the plane wave incidence angle. We compare different numerical approaches, including semi-analytic methods (high-frequency approximation coupled to ray modeling approach) and implicit methods (finite differences scheme). These different approaches have their own advantages and inconvenients, and domains of applicability. We analyze here how these methods can be complementary to understand the physical phenomenon that occurs during the reflection of a pulse by an immersed interface.

2 General overview of the problem

We consider here a plane interface separating a fluid and a solid medium. A point-like source is located in the fluid and generates an incident spherical wave (transient broadband signal) that is partially reflected in the fluid, and partially transmitted into the solid. In this paper, we only consider the reflected part of the acoustic field.

A point-like receiver (observation point) moves from the source position parallel to the interface, and we are interested in the computation of the transient signal measured at each position of the observer after reflection by the plane interface.

In the simple wavefront point of view, we expect to obtain the following contributions to the total reflected field in the fluid medium:

- Two spherical wavefronts, corresponding to the incident field and the so-called specular reflection,
- A conical wave, tangent to the specular reflection with an angle equal to the longitudinal critical angle (longitudinal head wave), this angle is characterized by the ratio c_f / c_l, where c_f is the velocity of acoustic waves in the fluid, and c_l is the longitudinal velocity in the solid,
- A second conical wave, tangent to the specular reflection with an angle equal to the transverse critical angle (transverse head wave), similarly this angle is characterized by the ratio c_f / c_t, where c_t is the transverse velocity in the solid,
- Another surface wave known as the leaky Rayleigh wave.

Here we are interested in the computation of the specular reflection and leaky Rayleigh wave, since the two head waves are generally very small compared to the former. This will be verified numerically using a finite difference scheme.

3 Computation of the reflected field

The plane interface is supposed to be located in the plane z=0, and the point-like source at x=y=0 and z=h>0. The impulse incident field generated by the source can be classically described as a diverging spherical wave (in terms of the velocity potential):

$$\Phi_i(x,y,z,t) = \frac{1}{4\pi R}\delta\left(t - \frac{R}{c_f}\right)$$

The computation of the reflected and transmitted fields is classically written for plane monochromatic waves. This is the reason why we start with a 1D Fourier transform over time of the transient incident field, followed by a 2D Fourier transform over the spatial variables x and y parallel to the interface ; this yields the decomposition of the incident field into plane monochromatic waves, that can be found as ref…

$$\tilde{\Phi}_i(f_x, f_y, z, f) \propto \frac{1}{f_z}\exp\left(2i\pi f_z |z-h|\right)$$

where f is the temporal frequency dual of time t, and f_x and f_y the spatial frequencies dual of x and y. The f_z coefficient can be understood as the spatial frequency along the z direction, and is obtained from the dispersion relationship in the fluid:

$$f_x^2 + f_y^2 + f_z^2 = f_r^2 + f_z^2 = f^2 / c_f^2$$

In the neighbourhood of the plane interface, $|z-h|$ can be replaced by $h-z$, therefore resulting in an incident wave that can be written as

$$\tilde{\Phi}_i(f_x, f_y, z, f) \propto \frac{1}{f_z}\exp(2i\pi f_z h)\exp(-2i\pi f_z z)$$

The presence of the interface generates a reflected field whose temporal and spatial frequencies f, f_x and f_y are unchanged ; compared to the incident field, this reflected part propagates in the opposite direction along the z axis and it can be formally written as

$$\tilde{\Phi}_r(f_x, f_y, z, f) \propto \frac{1}{f_z}\exp(2i\pi f_z h)\times R(\cdots)\times\exp(+2i\pi f_z z)$$

In this expression, $R(\cdots)$ corresponds to the reflection coefficient.

In the solid below the interface, the incident wave generates a transmitted longitudinal wave (L), and a vertically polarized transverse wave (TV). Both these components can be described in a similar manner that is not explicitly written here.

The boundary conditions that must be satisfied in the plane z=0 are:

- the continuity of the normal displacement,
- the continuity of the xz and zz components of the stress tensor.

Writing these three boundary conditions yields a complete solution of this problem, and allows to obtain the expression of the reflection coefficient $R(\cdots)$. Similarly, it is of course possible to calculate the transmission coefficients for the L and TV waves in the solid. Classically, the reflection coefficient $R(\cdots)$ only depends on the ratio f_x/f and f_y/f.

The last step consists in returning to the real physical space by an inverse 2D Fourier transform over f_x and f_y.

Formulating the inverse 2D Fourier transform over f_x and f_y as an angular integration, we obtain an integral along a complex path that starts at the origin $0+0i$ towards $\pi/2+0i$ (propagative components), and then continues towards $\pi/2-i\infty$ (evanescent components). A small change in the Fourier kernel allows to extend this integration path by symmetry with respect to the origin ; this ensures that the complex integration path is closed to infinity.

The Fourier kernel shows a phase that varies proportionally with the temporal frequency f. This yields the so-called semi-analytic approximation that corresponds to the high frequency assumption. In this case, the integral can be evaluated using the saddle-point method, that can be proved equivalent to the stationary phase theorem. Another formulation of this approximation can be written in terms of the Fermat principle, or minimum time of flight.

There is only one particular point on the complex integration path that makes the phase stationary ; this point corresponds to the specular reflection, that can be interpreted in the classical geometrical way (from the source to the interface, and the back to the observer, along a path that satisfies the first Snell's law). This contribution is characterized by a phase (or a time delay, its equivalent in the time domain), and a complex valued amplitude A_s (that results from the reflection coefficient). Used in conjunction with a transient excitation signal $s(t)$, this yields a specular reflected field that contains two terms: the first one is a replica of $s(t)$, with an amplitude given by the real part of A_s ; the second one is the Hilbert transform of $s(t)$, with an amplitude given by the imaginary part of A_s.

Using the stationary phase theorem yields a deformation of the integration path to an alternate path in the complex plane, along which the phase stationarity is satisfied. During this deformation, under some conditions we may go through a pole of the reflection coefficient ; the real part of this pole is very near the standard Rayleigh incidence, and its small imaginary part yields an exponential decrease of the corresponding contribution to the total reflected field. The influence of this pole can be evaluated in a closed form using the Cauchy integration method. This leads to a second term, that needs to be added to the specular reflection. Similarly, the second term is characterized by a phase (or time of flight) and complex amplitude. These two properties are then treated in the same manner as for the specular reflection.

Figure 1 illustrates how the complex integration path is changed using the stationary phase method (or equivalently the steepest descent approximation). The intersection of the steepest descent integration path with the real axis corresponds to the specular reflection from the source to the observation point.

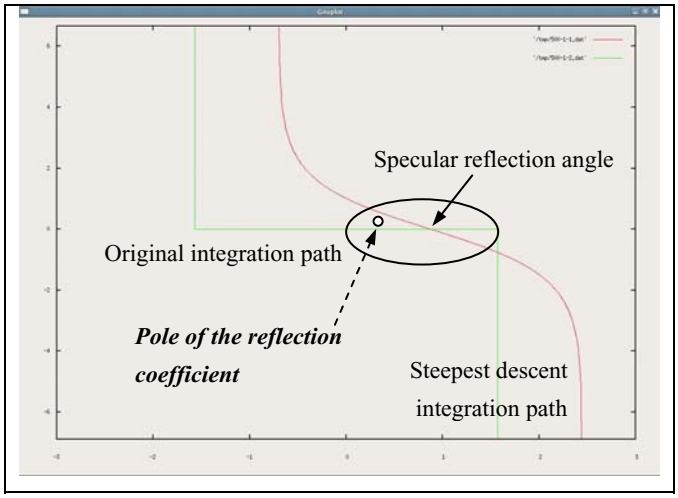

Figure 1: changing the integration path from the green to the red path encounters a pole of the reflection coefficient.

The second term resulting from the Cauchy integration around this pole corresponds to the leaky Rayleigh wave. Physically, it can be interpreted as a wave that propagates from the source to the interface with an incidence angle equal to the Rayleigh angle ; then we get a surface wave along the interface, that radiates energy in direction of the fluid along the Rayleigh angle again. This leaky Rayleigh wave can be observed only if the distance between the source and the observation point, measured parallel to the interface, is large enough.

These two contributions to the total reflected field are illustrated on figure 2: the red path corresponds to the specular reflection, and the yellow one to the leaky Rayleigh wave.

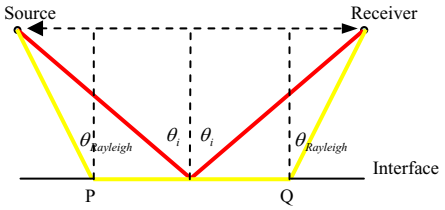

Figure 2: Specular reflection (red) and leaky Rayleigh wave (yellow).

From figure 2, we can easily predict that the leaky Rayleigh wave is observable if the distance d between the source and the receiver is larger than $2h\tan\theta_{Rayleigh}$ (if the receiver is located at a distance h above the interface).

Note that the longitudinal and transverse head waves are not taken into account in this description.

4 Software implementation

The first software, developed by D. Cassereau (P.A.S.S., Phased Array Simulation Software), is based on the semi-analytic approximation.

The second software, developed by E. Bossy (SimSonic), is based on a finite-difference time-domain numerical scheme. Figure 3 shows instantaneous views of the reflected (and transmitted) fields obtained by this method at different observation times 8, 16 and 28 µs. We clearly identify the incident wavefront and the specular reflection. In addition, we also clearly see the two head waves (small compared to the other components), and the leaky Rayleigh wave contribution.

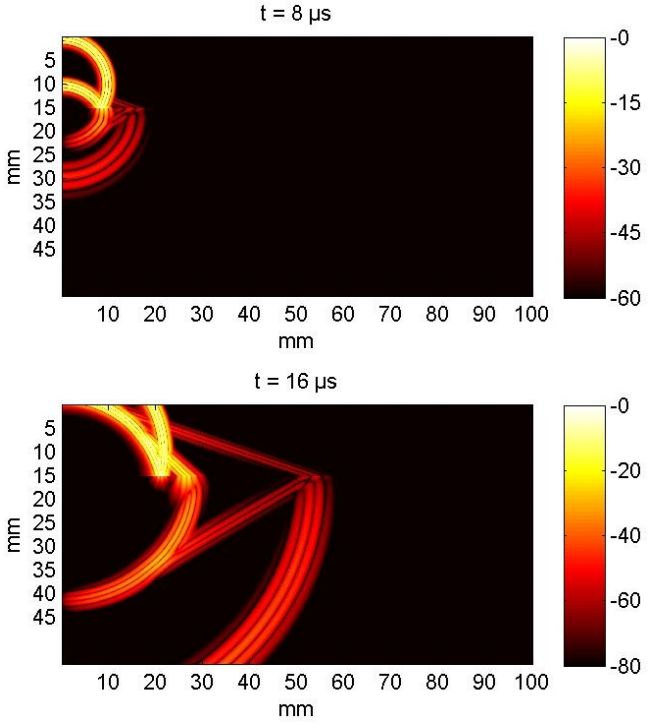

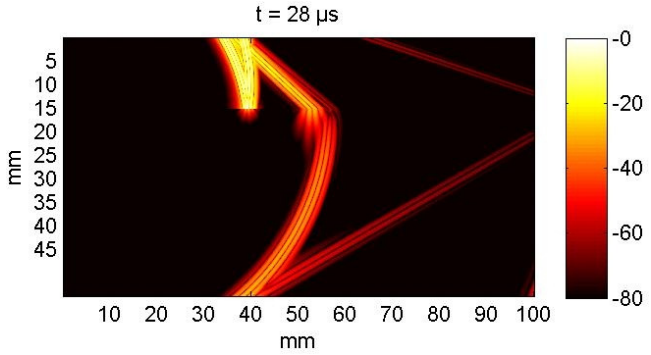

Figure 3: Results obtained with SimSonic at different times.

Figure 4 shows the echodynamic curve, the maximum amplitude of the temporal signal as the observer moves (the blue curve corresponds to SimSonic, and the red curve to P.A.S.S.). Both results match very well, except near 10 mm. This corresponds to the transverse critical angle, where the reflection coefficient varies fast with the incidence angle. In this case, semi-analytic methods do not yield pertinent results.

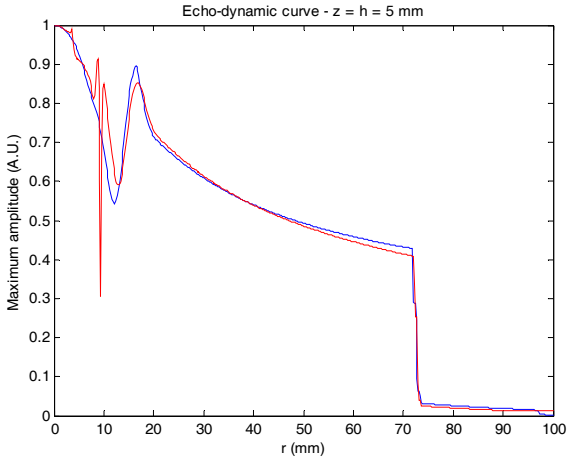

Figure 4: echodynamic curve ; comparison between SimSonic (red curve) and P.A.S.S. (blue curve)

Figure 5a shows the temporal signals calculated for a receiver located at a distance r=0, thus at the same position as the source. In this particular case, the leaky Rayleigh wave is not observable, and the reflected field reduces to the specular reflection pulse. We clearly see that the two simulations yields very similar results.

Figure 5b corresponds to an observation point located at r = 10 mm ; the results are no more similar, in amplitude nor in temporal signal shape. In this case, the semi-analytic method implemented by P.A.S.S. does not give very pertinent results, and this can be compared with the echodynamic curve shown on figure 4.

On figure 5c, the distance r is now equal to 20 mm and we clearly identify the leaky Rayleigh wave that appears before the specular reflection pulse. We also observe that the temporal shape of the leaky Rayleigh wave contribution differs from the one of the specular reflection.

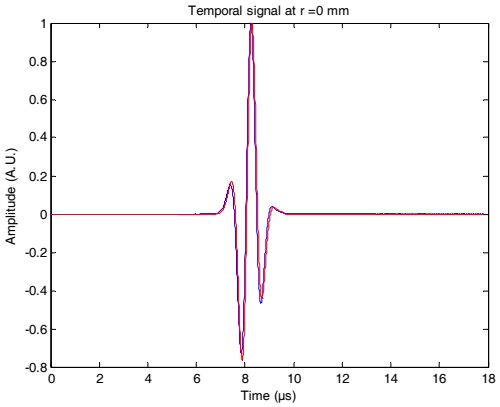

Figure 5a

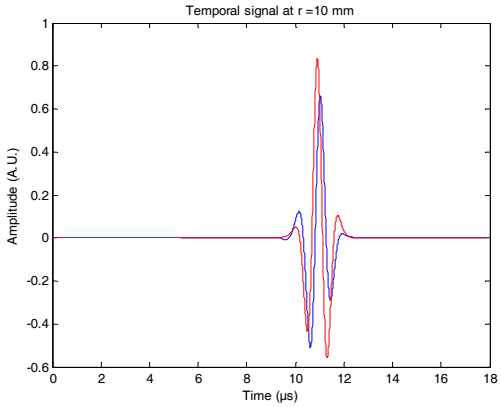

Figure 5b

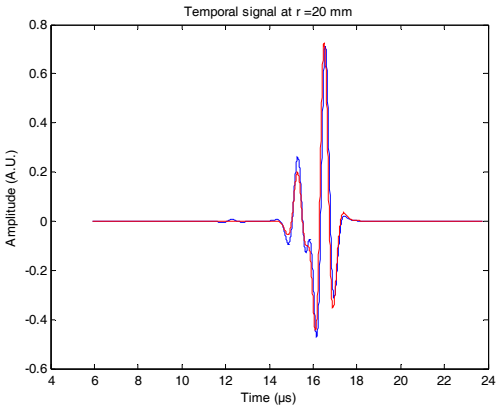

Figure 5c

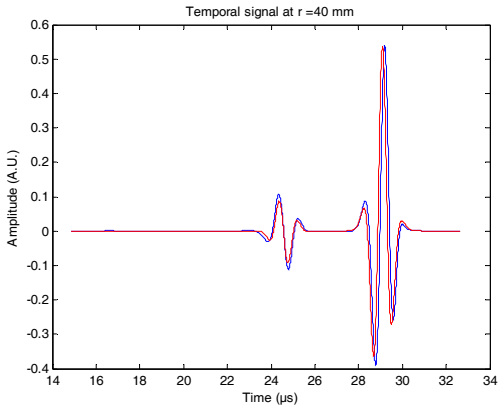

Figure 5d

Figure 5: temporal signals obtained at different positions of the receiver ; a) $r = 0$; b) $r = 10$ mm ; c) $r = 20$ mm ; d) $r = 40$ mm

It should be also noted that the two simulation methods provide again very similar results. The blue curve also shows a very small pulse at about 12 µs ; this corresponds to the transverse head wave that is of course present in the results from SimSonic, but not in those from P.A.S.S. We observe that this head wave contribution is very small compared to the leaky Rayleigh wave as well as the specular reflection.

Finally, figure 5d corresponds to a distance r equal to 40 mm: the two pulses are now very well separated in time. Once again, the two simulation methods provide very similar results, in signal amplitudes and temporal shapes.

5 Conclusion

The first objective of this work was to implement the computation of the leaky Rayleigh wave in a software like P.A.S.S. that is principally based on semi-analytic approximation of the propagation ; clearly this is a success, at least in the particular case of a plane interface between a fluid and a solid.

The second point of interest is that we could successfully compare the results obtained from two completely different simulation approaches, the first one based on an exact description of the propagation, and the second one based on the semi-analytic approach. Both methods have their own advantages and inconvenients, but they clearly converge to very similar results in most situations we have studied in this work.

References

[1] Physical Acoustics, Principles and Methods vol. X, Academic Press, pp. 1-21,

[2] I.S. Gradshteyn and I.M. Ryzhik, Table of Integrals, Series and Products, Academic Press,

[3] E. Bossy *et al.*, "Three-dimensional simulations of ultrasonic axial transmission velocity measurement on cortical bone models", J. Acoust. Soc. Am. **115**(5), pp 2314-2324 (2004),

[4] http://ia.loa.espci.fr/dc/pass.